THE JOURNAL OF CHEMICAL PHYSICS **138**, 034707 (2013)

Influence of the long-range corrections on the interfacial properties of molecular models using Monte Carlo simulation

J. M. Míguez,[1] M. M. Piñeiro,[1,a)] and Felipe J. Blas[2]
[1]*Departamento de Física Aplicada, Facultade de Ciencias, Universidade de Vigo, E36310 Vigo, Spain*
[2]*Departamento de Física Aplicada, Facultad de Ciencias Experimentales, Universidad de Huelva, E21071 Huelva, Spain*

(Received 20 November 2012; accepted 27 December 2012; published online 17 January 2013)

We analyze the influence of the long-range corrections, due to the dispersive term of the intermolecular potential energy, on the surface tension using direct simulation of the vapour-liquid interface of different molecular models. Although several calculation methods have been proposed recently to compute the fluid-fluid interfacial properties, the truncation of the intermolecular potential or the use of the tail corrections represents a contribution relevant from a quantitative perspective. In this work, a simplified model for methane, namely a spherical Lennard-Jones intermolecular potential, has been considered first, and afterwards other models including rigid non polarizable structures with both Lennard-Jones sites and point electric charges, representing some of the most popular models to describe water (namely the original TIP4P model, and the TIP4P/Ew and TIP4P/2005 versions), and carbon dioxide (MSM, EPM2, TraPPE, and ZD models) have been studied. Our results show that for all cases tested, including those in which the electrostatic interactions may be predominant, an incomplete account of the long-range corrections produces a systematic underestimation of the computed interfacial tension. © *2013 American Institute of Physics*. [http://dx.doi.org/10.1063/1.4775739]

I. INTRODUCTION

The prediction of thermodynamic and structural properties of molecular models comprising intermolecular dispersive interactions and long-range Coulombic forces, such as punctual charges for modelling electrostatic interactions, has been until recently a challenging problem especially for systems exhibiting any kind of inhomogeneity. In this particular case of inhomogeneous fluids, the treatment of the long-range corrections (LRCs) associated to the truncation of the potential of the dispersive forces presents some interesting subtleties. Although the effect of this truncation on different thermodynamic and structural properties might seem to be negligible, due to the small contribution of dispersive interactions if compared with electrostatic forces on the total energy, this is not the case for the surface tension. Since this property is one of the most sensitive magnitudes when it is calculated along a computer simulation run, a very precise evaluation of the inhomogeneous LRCs due to the dispersive interactions is necessary. Otherwise, the quantitative performance of a given molecular model to estimate interfacial properties might not be evaluated properly, yielding misleading conclusions. The objective of this paper is to study the influence of the LRCs, due to the dispersive interactions, on the surface tension of several realistic molecular models that combine dispersive and Coulombic interactions. In particular, we consider methane, which is described through the united-atom approach as a single Lennard-Jones (LJ) sphere, and water and carbon dioxide, which are treated as rigid non polarizable molecules containing several interacting sites, including both LJ dispersive interaction sites and punctual electric charges. An additional reason for the choice of these molecules is their undeniable applied interest in many fields, and in particular in the study of enhanced natural gas recovery and carbon dioxide stockage, in which their phase equilibria[1] and interfacial properties[2,3] play a key role. Moreover, the existence of very accurate experimental data for all the substances considered in this work allows to establish a comparison between the performance of different models for the same substance, evaluating the quantitative efficiency of each one in predicting interfacial properties.

Until very recently, there was not an easy, simple, and precise method for evaluating the LRCs due to the dispersive interactions in inhomogeneous systems. The first method intended to account for the LRCs was proposed by Chapela *et al.*,[4] and was later modified by Blokhuis *et al.*[5] Although this methodology provides a lower bound to the surface tension (and other thermodynamic properties), its main drawback is that it employs density profiles of the system determined without LRCs.

The first satisfactory methodology for dealing with LRCs for inhomogeneous systems was proposed by Guo and Lu,[6] a procedure extensively used later by Malfreyt and coworkers.[7–12] Although the method takes into account the LRCs to the energy and other properties, the presence of a non local term in the final expression involving an integral over density makes the procedure somewhat inconvenient for run time calculations. In addition to that, although the non local term seems to represent a relatively low contribution to the surface tension at low temperature, it becomes important close to the critical point.[13] For further details see the original work[6] and the review by MacDowell and Blas.[14]

a)Electrocnic mail: mmpineiro@uvigo.es

The same conceptual procedure accounting for the LRCs was recently proposed by Janeček,[13] based on related works of Mecke *et al.*[15,16] and Daoulas *et al.*[17] applied by several authors,[18–21] and later modified by MacDowell and Blas,[14] and de Gregorio *et al.*[51] The Janeček's method accounts very accurately for the LRCs in inhomogeneous systems along the whole range of temperatures in which the system exhibits vapour-liquid coexistence, and what is more important, the method has been shown to be very robust concerning the choice of the cutoff distance. A step further, the improved Janeček's method proposed by MacDowell and Blas[14] is able to evaluate in an exact way the intermolecular interactions without the need of computing the instantaneous density profile to calculate the LRCs to the intermolecular potential energy. With this new formulation, the method can be implemented in a compact and straightforward fashion in any standard Monte Carlo computer simulation code, since the final expression is given by an effective pairwise intermolecular potential between all the particles forming the system.[14] Another approach to the problem is the use of Ewald sums to deal also with dispersive interactions. This method has been applied by in 't Veld *et al.*[22] and Alejandre and Chapela,[23] but it is definitely much more complex from a mathematical point of view than other techniques, such as the Janeček's methodology. In addition to that, it is remarkably CPU time demanding, adding up to the already lengthy inhomogeneous simulation runs.

The rest of the paper is organized as follows. In Sec. II we consider an improved method for determining the LRCs of inhomogeneous systems. Molecular models and the simulation details of this work are presented in Sec. III. Results obtained are discussed in Sec. IV. Finally, in Sec. V we present the main conclusions.

II. IMPROVED JANEČEK'S METHODOLOGY: THE EFFECTIVE LONG-RANGE PAIRWISE POTENTIAL

In 2006, Janeček[13] proposed a new methodology for calculating the LRCs to the potential energy in systems that interact through spherically symmetric intermolecular potentials. This procedure allows to treat in a simple way the truncation of the intermolecular energy of systems that exhibit planar interfaces. More recently, MacDowell and Blas[14] have demonstrated that the Janeček's procedure can be rewritten into an effective long-range pair potential that allows a fast, easy, and compact implementation of method. Since the original and improved methodologies have been described elsewhere,[13,14,18] only a brief account of the most important details will be presented here.

Consider a system of N molecules contained in a volume V that interact through a pairwise intermolecular potential. The total intermolecular potential energy can be written as

$$U(r_{ij}) = \frac{1}{2}\sum_{i=1}^{N}\sum_{j=1}^{N} u(r_{ij}) = \frac{1}{2}\sum_{i=1}^{N} U_i, \tag{1}$$

where $u(r_{ij})$ is the intermolecular potential between particles i and j, that depends on the distance between the centres of molecules $r_{ij} \equiv |\mathbf{r}_i - \mathbf{r}_j|$, and U_i is the potential energy of molecule i due to the interactions with all molecules of the system. During a simulation, the potential energy of a particle is usually splitted into two contributions: one arising from the interaction of molecule i with all molecules inside a sphere of radius $r_c^{(i)}$ centered at this molecule, and a second term that corresponds to the interaction between the molecule i and the rest of molecules forming the system (i.e., all the molecules located outside the cutoff distance). The potential energy of a molecule i can be then written as

$$U_i = \sum_{j\in r_c^{(i)}} u(r_{ij}) + U_i^{\mathrm{LRC}}, \tag{2}$$

where $r_c^{(i)}$ is the so-called cutoff distance of particle i, the notation $j \in r_c^{(i)}$ denotes all the particles j located inside the cutoff sphere centered at the position of particle i, and U_i^{LRC} represents the intermolecular interactions between particle i and the rest of the system due to long-range corrections. Note that $r_c^{(i)} \equiv r_c$ since all molecules have actually the same cutoff distance.

In the original Janeček's methodology, the simulation box is divided into slabs parallel to the xy-plane (and to the planar interface), in such a way that if the width of these slabs is small enough the number density of the system $\rho(z)$ is approximately constant inside each of them. Here we have chosen the z axis as the direction perpendicular to the planar interface. If one assumes that the pair correlation function between two particles separated beyond the cutoff distance is equal to one, i.e., the distribution of particles separated a distance $r_{ij} \geq r_c$ is uniform, the intermolecular potential associated to the long-range correction, of a particle i located at position z_i (according to Janeček's original method[13]), is given by

$$U_i^{\mathrm{LRC}}(z_i) = \sum_{k=1}^{n_s} w(|z_i - z_k|)\rho(z_k)\Delta z, \tag{3}$$

where $\rho(z_k)$ is the density of the system in the slab of width Δz and centered at z_k, the index k runs for all the n_s slabs in which the simulation box is divided along the z axis, and $w(|z_i - z_k|)$ accounts for the intermolecular interactions due to the long-range correction between a particle i at z_i and all the particles located inside the slab centered at z_k and with a number density $\rho(z_k)$. The particular expression for $w(|z_i - z_j|)$ depends on the election of the intermolecular potential of the system. In the original Janeček's method, applicable for molecules interacting through the LJ intermolecular potential, the function $w(z)$ is given by

$$w(z) = \begin{cases} 4\pi\epsilon\sigma^2\left[\frac{1}{5}\left(\frac{\sigma}{r_c}\right)^{10} - \frac{1}{2}\left(\frac{\sigma}{r_c}\right)^{4}\right] & \text{if } z < r_c \\ 4\pi\epsilon\sigma^2\left[\frac{1}{5}\left(\frac{\sigma}{z}\right)^{10} - \frac{1}{2}\left(\frac{\sigma}{z}\right)^{4}\right] & \text{if } z > r_c \end{cases}. \tag{4}$$

The total contribution to the energy obtained from the long-range corrections is given then as a sum over individual contributions, with a factor of 1/2 to avoid including mutual interactions twice,

$$U^{\mathrm{LRC}} = \frac{1}{2}\sum_{i=1}^{N} U_i^{\mathrm{LRC}}(z_i). \tag{5}$$

Equations (3)–(5) constitute the original Janeček's method for estimating the energetic contribution due to long-range corrections. Although this method allows to calculate very accurately the long-range corrections of a LJ system that exhibits a planar interface, it has several drawbacks. The most important one is the calculation of the density profile on the fly, i.e., the need to recalculate the instantaneous density profile every step to be used in Eq. (3) and hence, to be able to calculate the tail corrections at each Monte Carlo step. Unfortunately, this makes the procedure cumbersome, especially in the case of molecular fluids,[14] and also complicated to code since the density profile must be updated at each Monte Carlo step. The improved methodology proposed recently by MacDowell and Blas[14] is simple and compact, and it is also easier to implement in a simulation code. The original Janeček's method assumes that $U_i^{\mathrm{LRC}}(z_i)$ is given by a discrete sum of n_s contributions due to each slab in which the simulation box is divided along the z axis (see Eq. (3)). In the improved procedure of MacDowell and Blas[14] Eq. (3) is given by the more accurate expression

$$U_i^{\mathrm{LRC}}(z_i) = \int_{-\infty}^{+\infty} w(|z_i - z|)\,\rho(z)\,dz, \tag{6}$$

where the discrete approximation given by Eq. (3) is replaced by the continuous expression of $U_i^{\mathrm{LRC}}(z_i)$. Using this formulation, the density profile of a system formed by N particles can be written formally as a summation of δ-Dirac distributions centered at the positions z_j, with $j = 1, \ldots, N$

$$\rho(z) = \frac{1}{\mathcal{A}} \sum_{j=1}^{N} \delta(z - z_j), \tag{7}$$

where $\mathcal{A}$ is the interfacial area of the xy-plane of the system. Note that the density is normalized appropriately since

$$\int_V \rho(z)\,dV = N. \tag{8}$$

Substituting Eq. (7) into Eq. (6) we have

$$U_i^{\mathrm{LRC}}(z_i) = \int_{-\infty}^{+\infty} w(|z_i - z|)\,\frac{1}{\mathcal{A}} \sum_{j=1}^{N} \delta(z - z_j)\,dz \tag{9}$$

and using the property of the δ-Dirac distribution, we obtain the final expression for $U_i^{\mathrm{LRC}}(z_i)$

$$U_i^{\mathrm{LRC}}(z_i) = \frac{1}{\mathcal{A}} \sum_{j=1}^{N} w(|z_i - z_j|). \tag{10}$$

Note that the sum in the previous equation runs over all the values of the index j ($j = 1, \ldots, N$), and this also includes the case $j = i$.

The total intermolecular interaction energy arising from the long-range corrections, given by Eq. (5), is then expressed as

$$U^{\mathrm{LRC}} = \frac{1}{2\mathcal{A}} \sum_{i=1}^{N} \sum_{j=1}^{N} w(|z_i - z_j|). \tag{11}$$

The unrestricted summation over indexes i and j can be finally transformed into a sum of pairwise effective (integrated) intermolecular potential over all the pairs of molecules in the system and N self-energy terms as

$$U^{\mathrm{LRC}} = \frac{1}{\mathcal{A}} \sum_{i=1}^{N-1} \sum_{j=i+1}^{N} w(|z_i - z_j|) + \frac{1}{2\mathcal{A}} \sum_{i=1}^{N} w(0). \tag{12}$$

The expressions given by Eqs. (10) and (12) are the key relationships of the improved version proposed by MacDowell and Blas:[14] the interaction energy due to the long-range corrections is given by an effective pairwise intermolecular potential between all the particles forming the system.

Each of the self-energy terms arising from the last contribution of Eq. (12) has a clear physical meaning that can be explained very easily by inspecting carefully Eq. (10). As previously mentioned, the intermolecular potential of particle i at z_i, due to the long-range corrections, includes N terms, being one of them a self-energy contribution arising from the case $j = i$ in Eq. (10). What is the physical meaning of this contribution? It is not for sure a truly self-energy term in the real sense since this has no physical reality. This is easily understandable since the function $w(z)$ is not a real intermolecular potential between two particles but an effective (integrated) potential. Focusing on Eq. (10), each contribution $\frac{1}{\mathcal{A}} w(|z_i - z_j|)$ (with $i = 1, \ldots, N$) represents the intermolecular potential, due to the interactions between the particle i with all the particles located inside the slab centered at z_j that are outside the cutoff sphere (i.e., due to the long-range interactions). Therefore, $w(0)$ represents the interaction of a given i particle with those others placed in the same density profile slab but located beyond the cutoff distance, and not a truly self-energy term in the real sense.

This procedure results in several important advantages over the original method: (1) Eqs. (10) and (12) correspond to the exact evaluation of the intermolecular interactions due to the long-range corrections. It is important to recall that the use of the original Janeček's version of the method implies a discretization of the simulation box along the z axis, which is in fact an approximation; (2) the improved procedure allows to evaluate U_i^{LRC} and U^{LRC} without the explicit calculation of the density profile on the fly, i.e., it is not necessary to update the density profile $\rho(z)$ at each Monte Carlo step. Just to give an order of magnitude, if the simulation of the vapour-liquid interface of a LJ system is equilibrated typically during 10^6 Monte Carlo cycles, and in each cycle we attempt to move N molecules ($N \sim 10^3$ molecules), the density profile of the system should be updated 10^9 times along the equilibration stage; (3) finally, the implementation of the method is straightforward. If one has a standard Monte Carlo code in the canonical ensemble, the only change needed is to include a new subroutine for the evaluation of the contribution to the total intermolecular energy due to the long-range corrections (at the start of the simulation), and an additional subroutine for calculating the contribution to the intermolecular energy of a given particle due to the long-range corrections (each time a molecule displacement is attempted).

III. MOLECULAR MODELS AND SIMULATION DETAILS

In this work we investigate the effect of LRC due to the dispersive interactions on the interfacial properties of

three different molecular systems, methane, water, and carbon dioxide. There are several reasons for this choice. As it will be detailed, methane is usually described as a single LJ sphere, while the molecular models for water and carbon dioxide combine LJ sites and Coulombic interactions described through punctual electric charges. This will allow to establish a comparison between the influence and relative weight of the LRCs for both types of interactions in the determination of interfacial properties. In a previous work,[24] the influence of the method used to account for Coulombic interactions in the calculation of interfacial properties for various water models was analyzed, showing the equivalence between Ewald summation and the reaction field (RF) method in this application. Therefore, we evaluate now the effect of the LRCs due to the dispersive interactions on different interfacial properties, with special emphasis on surface tension.

Methane is modelled, following the united-atom approach, as a single LJ sphere to account for, in an effective way, the nearly spherically symmetric dispersive interactions.[25,26] For the case of carbon dioxide, the most usual model is a linear-rigid chain molecule with three chemical units, representing each of the C and O atoms, and each unit or interacting site consists of a combination of a LJ site plus an electric point charge. The molecule is considered to be rigid and non polarizable. This structure mimics the typical anisotropic feature of carbon dioxide, including the large quadrupole moment value accounted for the three partial charges. Among the available parametrizations for this molecular structure, in this case the original version of the MSM[27–29] model, named after the initials of the authors of the original paper, as well as those denoted as EPM2[30] (a variation of the original EPM, standing for elementary physical model), TraPPE[31] (transferable potentials for phase equilibria), and ZD (Zhang and Duan[32]) models, were tested. In the case of water, the well-known original TIP4P molecular model[33] and two modifications of it, the TIP4P/Ew[34] and TIP4P/2005[35] models, were also studied. All of them share the same site definition and molecular geometry: four interacting centers, with the oxygen atom O as the only LJ interaction site, a partial charge (M-site) located along the H-O-H angle bisector, and two hydrogen atoms H, which are represented by partial point electric charges. Table I summarizes the characteristic parameters for all the molecular models studied in this work.

Following the ensuing discussion, the pairwise intermolecular potential between molecules i and j may now be written as

$$u(r_{ij}) = \sum_{a=1}^{n_a} \sum_{b=1}^{n_b} u_{ab}(r_{ab}), \tag{13}$$

where n_a and n_b are the numbers of sites in the molecules i and j, respectively. $u_{ab}(r_{ab})$, the interaction potential between two sites of molecules i and j, is given by,

$$u_{ab}(r_{ab}) = 4\epsilon_{ab}\left[\left(\frac{\sigma_{ab}}{r_{ab}}\right)^{12} - \left(\frac{\sigma_{ab}}{r_{ab}}\right)^{6}\right] + \frac{1}{4\pi\epsilon_0}\frac{q_a q_b}{r_{ab}}, \tag{14}$$

TABLE I. Lennard-Jones potential well depth ϵ and size σ, partial charges q, and geometry, of the CH_4, H_2O, and CO_2 models used.

Atom	ϵ/κ(K)	σ(Å)	$q(e)$	Geometry
CH_4[25,26]	149.92	3.7327	0	
TIP4P H_2O[33]				
O	78.0	3.154	0.0	O-H: 0.9572 Å
H	0.0	0.0	0.52	O-M: 0.15 Å
M	0.0	0.0	− 1.04	H-O-H: 104.5°
TIP4P/Ew[34] H_2O				
O	81.9	3.16435	0.0	O-H: 0.9572Å
H	0.0	0.0	0.52422	O-M: 0.125 Å
M	0.0	0.0	− 1.04844	H-O-H: 104.5°
TIP4P/2005[35] H_2O				
O	93.20	3.1589	0.0	O-H: 0.9572 Å
H	0.0	0.0	0.5564	O-M: 0.1546 Å
M	0.0	0.0	− 1.1128	H-O-H: 104.52°
MSM[27–29] CO_2				
C	29.0	2.785	0.5957	C-O: 1.16 Å
O	83.1	3.014	− 0.29785	O-C-O: 180°
EPM2[30] CO_2				
C	28.129	2.757	0.6512	C-O: 1.149 Å
O	80.507	3.033	− 0.3256	O-C-O: 180°
TraPPE[31] CO_2				
C	27.0	2.80	0.70	C-O: 1.16 Å
O	79.0	3.05	− 0.35	O-C-O: 180°
ZD[32] CO_2				
C	28.845	2.7918	0.5888	C-O: 1.163 Å
O	82.656	3.0	− 0.2944	O-C-O: 180°

where r_{ab} is the distance between interacting sites a and b in molecules i and j, respectively, σ_{ab} and ϵ_{ab} are the size and dispersive energy parameters associated to the LJ dispersive interactions between a pair of a and b sites in these molecules, and q_a and q_b are the partial charges on these sites, with ϵ_0 the vacuum permittivity. Note that in the case of interactions involving methane, the Coulombic term is always equal to zero. The unlike LJ parameters ϵ_{ab} and σ_{ab} are given by the Lorentz-Berthelot combining rules,

$$\epsilon_{ab} = \sqrt{\epsilon_{aa}\epsilon_{bb}}, \tag{15}$$

$$\sigma_{ab} = \frac{1}{2}\left(\sigma_{aa} + \sigma_{bb}\right), \tag{16}$$

where σ_{kk} and ϵ_{kk} are the LJ size and dispersive energy parameters of a k-type interacting site, respectively.

Molecular simulations were initially started from a cubic box of size $L_x = L_y = L_z > 10\sigma$, where σ stands for the typical size of each molecular model used in this work. Systems containing $N = 1024$ molecules were equilibrated at constant temperature and pressure, in the isothermal-isobaric or NPT ensemble. Typically, the system was equilibrated, starting from an initial bcc ordered configuration, during 5×10^6 Monte Carlo cycles. Once the system was equilibrated, the original cubic box containing the system was placed between two equal size empty boxes added at both sides along the z direction. The simulations continued then in the NVT canonical ensemble. At temperatures below the critical

temperature, the system spontaneously develops two parallel vapour-liquid interfaces perpendicular to the z axis of this biphasic simulation box, allowing to study the properties of interest, including surface tension and interfacial thickness, among others.

The *NPT* and *NVT* Monte Carlo simulations were organized in cycles. Each cycle consisted of N attempts of displacement (translation, and also rotation in the case of non-spherical molecular models) of a molecule selected at random, plus one volume change try in the case of *NPT* simulations. The type of move was selected randomly with fixed probabilities. The acceptance ratios for translational, rotational moves, and volume changes were tuned to approximately 30%. Minimum image convention and periodic boundary conditions were considered. The simulation box was divided into 100 parallel slabs along the z axis in order to calculate the vapour-liquid density profile. In the biphasic simulations, after an initial equilibration period of 5×10^5 cycles, we generated typically 2×10^6 additional cycles to accumulate averages of the desired interfacial properties. The uncertainties of the simulated results were obtained using block averaging, by dividing the simulation run in ten subsets.

The total LJ contribution to the intermolecular interaction energy was computed using two different approaches. The first one entailed the use of a spherical cutoff distance (r_c) to truncate the interaction, considering no LRCs, i.e., neglecting the contribution to the intermolecular potential energy of pairs of molecules separated by a distance larger than this cutoff value. The second method consisted in the use of a spherical cutoff distance (r_c) for each interacting site, considering as distance scaling unit the σ value for that particular site, using the LRCs evaluation method proposed by Janeček[13] following the improved formulation of MacDowell and Blas.[14] This allowed us to determine the relevance of this particular term in the calculation of interfacial properties.

In this work we also use two different approaches to account for the Coulombic interactions, i.e., the reaction field methodology and the Ewald sums. Here we only explain the most important features of both techniques. In the reaction field (RF) method, the same cutoff distance is used as that for the LJ interactions. In this case, the Coulombic interaction energy between two point charges, u_{coul}, is computed as follows:

$$u_{coul} = \frac{q_a q_b}{4\pi\epsilon_0 r_{ab}} \left[1 + \frac{\epsilon_{RF} - 1}{2\epsilon_{RF} + 1} \left(\frac{r_{ab}}{r_c} \right)^3 \right], \tag{17}$$

where ϵ_{RF} is the dielectric constant of the surrounding media. In the case of water, the value $\epsilon_{RF} = 78.5$ has been used, which is valid for moderately to highly polar liquids, while for carbon dioxide the considered value is $\epsilon_{RF} = 1.66$. In a previous work[24] it has been shown that the use of the RF method yields analogous results than the Ewald sums method (within the simulation statistical uncertainty) for calculating the interfacial tension of these molecular models of water.

In the Ewald sums approach,[36] the total electrostatic energy of a system of N point charges q_a placed at positions r_a can be written as

$$U_{coul}(r_{ab}) = \frac{1}{2V} \sum_{k \neq 0} \frac{4\pi}{k^2} |\rho(k)|^2 \exp\left(-\frac{k^2}{4\alpha} \right) - \left(\frac{\alpha}{\pi} \right)^{\frac{1}{2}} \sum_{a=1}^{N} q_a^2 + \frac{1}{2} \sum_{a \neq b}^{N} \frac{q_a q_b (\sqrt{\alpha} r_{ab})}{r_{ab}}, \tag{18}$$

where

$$\rho(k) = \sum_{a=1}^{N} q_a \exp(i k r_a), \tag{19}$$

where V is the volume of the unit cell, given by $L_x \times L_y \times L_z$, α is the Ewald screening parameter, and $\mathbf{k}$ is a reciprocal lattice vector given by $(2\pi n_x/L_x, 2\pi n_y/L_y, 2\pi n_z/L_z)$, with n_x, n_y, n_z integers. In the calculations, α and the number of $\mathbf{n}$ and $\mathbf{k}$ vectors are adjustable parameters, and their values are typically selected to achieve the optimum computational efficiency.

Average density profiles were calculated during the simulations and fitted to a hyperbolic tangent function as

$$\rho(z) = \frac{\rho_l - \rho_v}{2} - \frac{\rho_l - \rho_v}{2} \tanh\left(\frac{z - z_0}{d} \right), \tag{20}$$

where ρ_l, ρ_v, z_0, and d are the liquid and vapour coexistence densities, the position of the Gibbs-dividing surface, and the width of the interface, respectively. The liquid and vapour densities were determined using the average density profile at each temperature and d was obtained from the hyperbolic tangent function. The "10-90" thickness value of the interface, t, is related to d by $t = 2.1972d$.

The surface tension of the simulated planar interface was computed using the mechanical and thermodynamic routes. In the first case, the interfacial tension is calculated from the diagonal components of the pressure tensor,

$$\gamma = \frac{L_z}{2} \left[\langle P_{zz} \rangle - \frac{\langle P_{xx} \rangle + \langle P_{yy} \rangle}{2} \right], \tag{21}$$

where L_z is the length of the simulation box along the z axis, perpendicular to the interface, and $P_{\alpha\alpha}$, with $\alpha = x, y, z$, are the diagonal components of the pressure tensor, which in this case were determined following the perturbative method proposed by de Miguel and Jackson.[37]

In the second case, namely, the thermodynamic route, the test-area (TA) technique proposed by Gloor *et al.*[38] was used to determine the interfacial tension during the simulation performing virtual changes of the interfacial area of the simulation cell. Following the original work, the surface tension can be calculated as

$$\gamma = \lim_{\Delta\mathcal{A} \to 0} \left(\frac{\Delta A_{0 \to 1}}{\Delta\mathcal{A}} \right)_{N,V,T} = -\frac{k_B T}{\Delta\mathcal{A}} \ln \left\langle \exp\left(\frac{-\Delta U}{\kappa_B T} \right) \right\rangle_0, \tag{22}$$

where k_B is the Boltzmann constant, $\Delta\mathcal{A}$ represents a small change in the interfacial area keeping the volume constant, and ΔU is the change in the configurational energy associated to this perturbation. The TA method has become very popular due to its versatility and it has been applied by different

authors to determine the vapour-liquid interfacial properties of LJ chains,[39] several water models,[40] the Mie potential,[41] binary fluid mixtures,[3,11] and recently it has been used to determine the solid-fluid interfacial tension of a confined LJ fluid.[42]

Nevertheless, the results of these calculations are in any case greatly dependent of the type of LRCs used for each term of the intermolecular potential, and this also concerns the LJ dispersive interactions. Assuming the equivalence of the RF and Ewald sums methodologies to account for the long-range Coulombic interactions, as previously demonstrated[24] for this particular simulation setup, the objective now is to determine the effect of the LRCs, due to the dispersive interactions, on the interfacial properties. Here we are particularly interested on the comparison of two approaches. In the first case, the LJ contribution to the intermolecular interactions was computed with a spherical cutoff distance with no further correction. An estimate of the tail correction to the surface tension due to the truncation of the LJ interaction may be calculated *a posteriori*. Once the simulation has finished, the hyperbolic tangent approximation given by (Eq. (20)) can be used to fit the density profile obtained from simulation and calculate the tail correction to the surface tension as[4,43]

$$\gamma_{tail} = 12\pi\epsilon\sigma^6(\rho_l - \rho_v)^2 \int_0^1 ds \int_{r_c}^{\infty} dr \times \coth\left(\frac{rs}{d}\right)\left(\frac{3s^3 - s}{r^3}\right). \quad (23)$$

The two-dimensional integral can be solved numerically in a 2D grid of points covering the range indicated by the limits of the integral. A sensitivity analysis has been performed in order to determine the trend of the integral value depending on the step of the grid in each direction. The final value has been found to be convergent beyond a certain step value.

In the second case, we used a proper LRC evaluation method to account for the neglected part of the intermolecular potential energy using the technique proposed by Janeček and improved by MacDowell and Blas as described in Sec. II.

IV. RESULTS

We first consider the simple molecular model of methane. In particular, we focus our attention on the influence of the cutoff distance and the treatment of the LRCs, due to the dispersive interactions, on the determination of the phase coexisting densities and interfacial properties. The surface tension has been evaluated using two different routes, the TA method and the mechanical route.

As can be seen in Table II, the effect of the cutoff distance on the vapour-liquid coexistence densities is very important, particularly in the case of the vapour density. The density value obtained using a cutoff distance of $r_c = 2.5\sigma$ is 70% larger than the corresponding values obtained using LRCs. It is worth noting that for the case of the larger cutoff value shown in this Table, $r_c = 8\sigma$, simulations were performed in a box of initial dimensions $L_x = L_y = 60\sigma$, containing 2662 methane molecules, in order to respect the ratio between the cutoff distance and the box size. The trend of the coexistence density values with the increasing cutoff distance can be seen clearly in Table II, showing that results obtained without LRCs are only consistent for cutoff distances equal or larger than 5σ. This result is coincident with the analysis performed by Trokhymchuck and Alejandre[44] for the LJ fluid using both MC and molecular dynamics simulations. On the other hand, a cutoff distance of only $r_c = 3\sigma$ is enough to obtain the same results if a proper treatment of the LRCs is considered. This tendency is also represented in Figs. 1(a) and 1(b) for coexistence density and interfacial tension, respectively. This result represents, besides the guarantee to obtain a reliable and exact property value for the molecular model explored, a considerable saving in CPU time in calculations that, as already said, are highly time demanding. It is worth mentioning that the differences between the experimental value and predictions from simulation are larger when LRCs are used. This must be taken into account since an incomplete account of the LRCs may produce misleading conclusions about the quantitative performance of a given molecular model parametrization. In this particular case, the fact that most forcefields are tuned to reproduce the dense fluid phases behaviour is also to be born in mind, especially for the dense liquid phase for which the LRC corrected value is slightly better.

TABLE II. Simulation data of coexisting densities (ρ_l and ρ_v, both in kg m^{-3}) for the Lennard-Jones methane model at 120 K and different cutoff radius values.

	NO-LRC		Janeček-LRC	
r_c/σ	ρ_l	ρ_v	ρ_l	ρ_v
2.5	390.7(4)	5.58(7)	405.6(4)	3.15(5)
3	399.3(4)	4.36(5)	407.5(7)	3.05(6)
4	402.3(3)	3.70(5)	407.9(7)	3.05(8)
5	406.2(7)	3.29(7)	407.5(7)	3.08(4)
8	406.4(6)	3.25(6)	407.6(8)	3.07(5)
Exp.[45]	410.01	3.24	410.01	3.24

Similar results are obtained for the surface tension of methane. As can be seen in Table III and Fig. 1(b), the effect of using a cutoff distance (without LRCs) is negligible when its value is larger than 5σ. However, to obtain the same cutoff independent predictions, only a cutoff distance of $r_c = 3\sigma$ is necessary if LRCs are used. Differences between the results obtained with LRC and without them (using $r_c = 2.5\sigma$) are around 30% approximately. Note also that predictions from simulations for the surface tension using the TA and mechanical routes produce compatible numerical values, as expected. Finally, two interesting features can be mentioned here. First, the tail correction for interfacial tension determined through the integral in Eq. (23) has also been calculated and presented in the column denoted as tail-LRC in Table III. The results show that this term value depends on the cutoff distance used during the simulation, and leads to a final interfacial tension value that does not show monotonic convergence with increasing cutoff distance, contrarily to what happened in the other cases, indicating clearly a limited reliability of this methodology when accounting for the LRCs. Second, the interfacial tension value obtained without LRCs is closer to

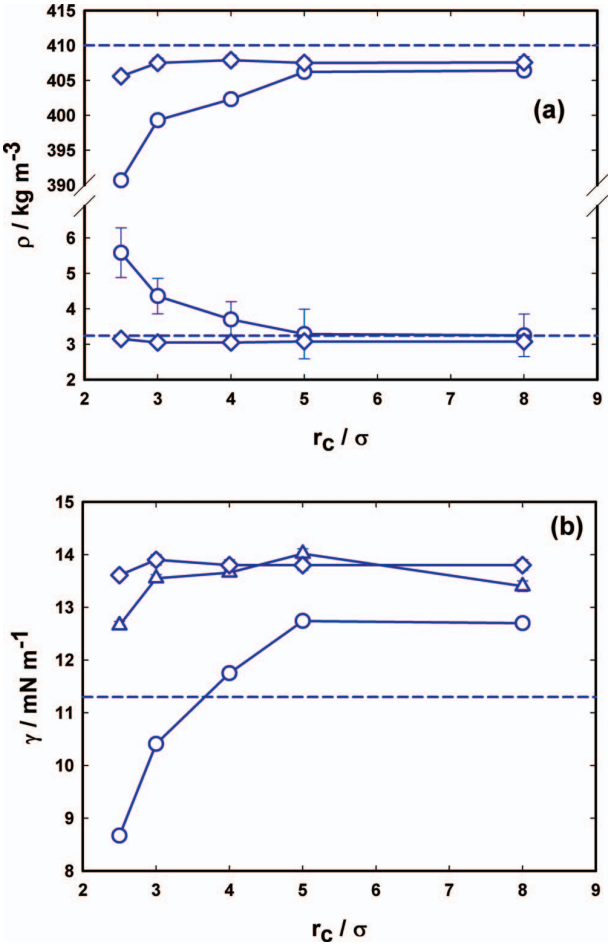

FIG. 1. (a) Evolution with the cutoff radius value of the computed coexisting densities (liquid phase above, gas phase below) for LJ methane at 120 K. Circles: calculation without LRCs. Diamonds: calculation with Janeček's LRCs. In both cases the dashed line represents the NIST recommended experimental value. (b) id for computed interfacial tension, computed using the TA method. In this case triangles represent the values obtained applying the LRCs represented by Eq. (23).

the experimental value than that corresponding to the LRC value, what might induce misleading conclusions about the performance of a given molecular model. As in the case of coexistence densities, the ability of a given model for predicting quantitatively the surface tension must be evaluated with care, through a complete calculation that takes into account LRCs in order to obtain the "real" model value for the point considered. Indeed, the correct treatment of LRCs in inhomogeneous simulations can be used as a demanding test to evaluate the quality of a given force field parametrization. Note that the interfacial tension containing the complete LRC treatment is around 7% higher than the non-corrected value obtained with the largest cutoff value tested, which is significative from a quantitative point of view. It is also important to remark that this value overestimates the experimental value.

Once the influence of the LRCs, due to the dispersive interactions, on the phase behaviour and interfacial properties for a model consisting of a single LJ site (methane) has been evaluated, we consider now the case of a molecular

TABLE III. Simulation data of surface tension (γ in mJ m^{-2}) for the Lennard-Jones methane model at 120 K and different cutoff radius values. Subscripts *ta* and *mr* stand for test area and mechanical route, respectively.

	NO-LRC		tail-LRC		Janeček-LRC	
r_c/σ	γ_{ta}	γ_{mr}	γ_{ta}	γ_{mr}	γ_{ta}	γ_{mr}
2.5	8.67(7)	8.67(7)	12.66(7)	12.66(7)	13.61(7)	13.64(7)
3	10.41(7)	10.41(7)	13.55(7)	13.55(7)	13.9(1)	13.8(1)
4	11.75(9)	11.75(9)	13.66(9)	13.66(9)	13.8(1)	13.8(1)
5	12.74(9)	12.73(9)	14.03(9)	14.02(9)	13.8(1)	13.8(1)
8	12.7(1)	12.7(1)	13.4(1)	13.4(1)	13.7(1)	13.8(1)
Exp.[46]			11.3			

model that also includes Coulombic interactions such as water. Table IV shows the coexisting densities as obtained from Monte Carlo simulations at a single temperature, 400 K, for the TIP4P/2005 model.[35] We have used different methods for calculating both the dispersive interactions associated to the LJ potential and the Coulombic interactions due to the presence of point charges in the molecular model. In particular, we neglect the LRCs associated to the dispersive interactions and calculate explicitly the LRCs using the Janeček's methodology. In addition to that, we have also computed the Coulombic interactions using two different procedures, the Ewald sums and the RF method. The results show that in the case of molecular models with electrostatic interactions the effect of truncation of dispersive LJ interactions on the coexisting densities is less pronounced than in systems with only LJ interactions. As in the case of methane, the use of LRCs allows to choose shorter values of r_c, but the differences between both results are not relevant, as can be seen clearly in Fig. 2(a). However, this is no longer true for the case of the interfacial tension, as it is shown in Table V and Fig. 2(b). The value of the surface tension obtained using the LRCs is approximately 7% higher than that obtained when LRCs are disregarded, obtaining a better agreement between simulation predictions and experimental data taken from literature. It is obvious from these results that the surface tension is much more sensitive to LRCs than the coexisting densities. As in the case of methane, the use of LRCs *a posteriori* (tail-LRC) yields a somewhat erratic trend.

TABLE IV. Simulation data of coexisting densities (ρ_l and ρ_v, both in kg m^{-3}) for the TIP4P/2005 water model at 400 K and different cutoff radius values.

	NO-LRC		Janeček-LRC			
r_c/σ	ρ_l	ρ_v	ρ_l^{RF}	ρ_v^{RF}	ρ_l^{EW}	ρ_v^{EW}
1.5			948(3)	0.53(4)		
2			946(2)	0.70(3)	947(2)	0.66(4)
2.5	924(2)	0.65(3)	935(2)	0.56(2)	935(2)	0.59(3)
3	926(2)	0.56(4)	929(1)	0.57(4)	928(2)	0.57(4)
4	929(2)	0.60(2)	929(1)	0.58(3)	928(2)	0.57(4)
5	929(1)	0.60(3)	929(2)	0.58(3)	928(2)	0.57(5)
Exp.[47]	937.5	1.37	937.5	1.37	937.5	1.37

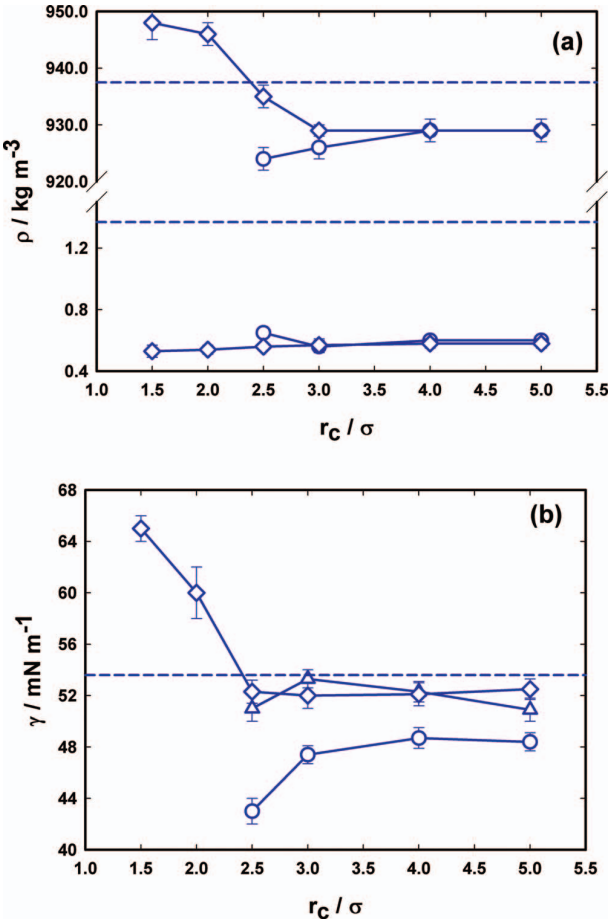

FIG. 2. Same caption as Figure 1, for TIP4P/2005 water molecular model, at 400 K. For the points represented, the RF method was used to handle electrostatic interactions.

Before finishing the analysis of the effect of the LRCs on the properties of water, it is important to mention that the values obtained for both coexisting densities and surface tension values, are identical using Ewald sums and RF methods for determining the Coulombic interactions of the system. Also, as in the case of methane, the surface tension values obtained using the TA methodology and the mechanical route are identical to within the statistical errors of the simulation results. Taking into account this information, and unless otherwise stated, the rest of the interfacial tension data reported in this work were obtained using TA technique and RF method. In addition to that, we have used the cutoff distance value of $r_c = 3\sigma$ for calculating the LRCs under the Janeček's approximation.

TABLE VI. Simulation data of coexisting densities (ρ_l and ρ_v, both in kg m^{-3}) and surface tension (γ/ mJ m^{-2}), for the different water molecular models tested. The reaction field method was used in the simulations to handle electrostatic interactions, and a constant LJ cutoff radius $r_c = 3\sigma$ was used. These values are compared with experimental values.

T/K	ρ_l^{LRC}	ρ_l^{NIST}	ρ_v^{LRC}	ρ_v^{NIST}	$\gamma_{ta}^{\mathrm{LRC}}$	γ^{NIST}
			TIP4P/2005			
350	968(1)	973.7	0.09(2)	0.26	60.9(9)	63.2
400	929(2)	937.5	0.58(3)	1.37	52(1)	53.6
450	882(2)	890.3	2.3(2)	4.8	41(1)	42.9
500	820(2)	831.3	7.4(3)	13.2	30(2)	31.5
			TIP4P/Ew			
350	963(3)	973.7	0.11(2)	0.26	56(2)	63.2
400	922(2)	937.5	0.9(1)	1.37	45.9(7)	53.6
450	869(2)	890.3	3.2(2)	4.8	35.8(9)	42.9
500	799(2)	831.3	10.1(3)	13.2	27(1)	31.5
			TIP4P			
350	953(2)	973.7	0.32(3)	0.26	48(1)	63.2
400	896(2)	937.5	1.9(1)	1.37	37.5(9)	53.6
450	827(2)	890.3	7.3(2)	4.8	27.5(8)	42.9
500	732(2)	831.3	26(1)	13.2	16(1)	31.5

We have also determined the vapour-liquid coexisting densities and the surface tension of different models of water, including TIP4P/2005, TITP4P/Ew, and the original TIP4P, at several temperatures, from 350 up to 500 K. Results obtained are presented in Table VI. The experimental data values recommended by the NIST, the Setzmann and Wagner[45] dedicated EoS for the case of coexistence densities and Somayajulu[46] EoS for interfacial tension, are also listed in the table. As can be seen, the TIP4P/2005 model provides the best description of these properties, as previously established.[40]

Finally, we have analysed the effect of the LRCs, due to the dispersive interactions, on the phase behaviour and interfacial properties of carbon dioxide. In particular, we consider here several models of CO_2 that describe this molecule as a linear rigid trimer with three LJ sites and three point

TABLE V. Simulation data of surface tension (γ in mJ m^{-2}) for the TIP4P/2005 water model at 400 K and different cutoff radius values. Subscripts *ta* and *mr* stand for test area and mechanical route, respectively.

	NO-LRC		tail-LRC		Janeček-LRC			
r_c/σ	γ_{ta}	γ_{mr}	γ_{ta}	γ_{mr}	γ_{ta}^{RF}	γ_{mr}^{RF}	γ_{ta}^{EW}	γ_{mr}^{EW}
1.5					65(1)	64(2)		
2					60(2)	60(1)	58(1)	57.2(9)
2.5	43(1)	42(1)	51(1)	50(1)	52.3(9)	53(1)	53.7(7)	54(1)
3	47.4(7)	47.9(7)	53.3(7)	53.8(7)	52(1)	51.8(8)	52(1)	52(1)
4	48.7(8)	48.6(8)	52.3(8)	52.1(8)	52.1(9)	52.3(9)	52(1)	52.2(8)
5	48.4(7)	48.4(9)	50.9(7)	50.9(9)	52.5(8)	52(1)	52(1)	52.2(8)
Exp.[48]				53.6				

TABLE VII. Simulation data of coexisting densities (ρ_l and ρ_v, both in kg m^{-3}) for the different CO_2 molecular models tested. The reaction field method was used in the simulations to handle electrostatic interactions, and a constant LJ cutoff radius $r_c = 3\sigma$ was used. These values are compared with NIST recommended values (Span and Wagner[49]).

T/K	$\rho_l^{\text{NO-LRC}}$	ρ_l^{LRC}	ρ_l^{NIST}	$\rho_v^{\text{NO-LRC}}$	ρ_v^{LRC}	ρ_v^{NIST}
			MSM			
230	1110(1)	1121(1)	1129	28.4(4)	24.2(3)	23.3
240	1071(2)	1083(1)	1089	38.5(3)	35.8(4)	33.3
250	1029(1)	1042(2)	1046	55.4(2)	49.8(5)	46.6
260	982(2)	995(2)	999	73.0(6)	67.6(5)	64.4
270	927(1)	943(2)	946	100.4(7)	90.2(7)	88.4
			EPM2			
230	1113(2)	1123(3)	1129	27.5(2)	24.9(2)	23.3
240	1075(2)	1084(2)	1089	38.5(5)	34.6(4)	33.3
250	1027(2)	1040(2)	1046	54.1(4)	48.0(6)	46.6
260	978(1)	994(2)	999	76.3(5)	69.1(3)	64.4
270	922(1)	940(1)	946	103.9(7)	93.6(5)	88.4
			TraPPE			
230	1117(2)	1124(2)	1129	23.1(2)	20.4(3)	23.3
240	1080(3)	1083(2)	1089	33.1(4)	31.4(2)	33.3
250	1037(1)	10\(2)	1046	46.2(5)	42.6(3)	46.6
260	990(2)	1002(2)	999	64.4(5)	56.9(7)	64.4
270	936(1)	954(2)	946	89.2(6)	78.2(5)	88.4
			ZD			
230	1118(2)	1126(1)	1129	28.9(3)	25.9(3)	23.3
240	1078(2)	1088(2)	1089	40.5(4)	36.5(2)	33.3
250	1031(1)	1045(2)	1046	57.8(5)	51.2(7)	46.6
260	981(1)	998(1)	999	79.6(5)	70.8(4)	64.4
270	927(1)	944(1)	946	105.1(9)	93.3(4)	88.4

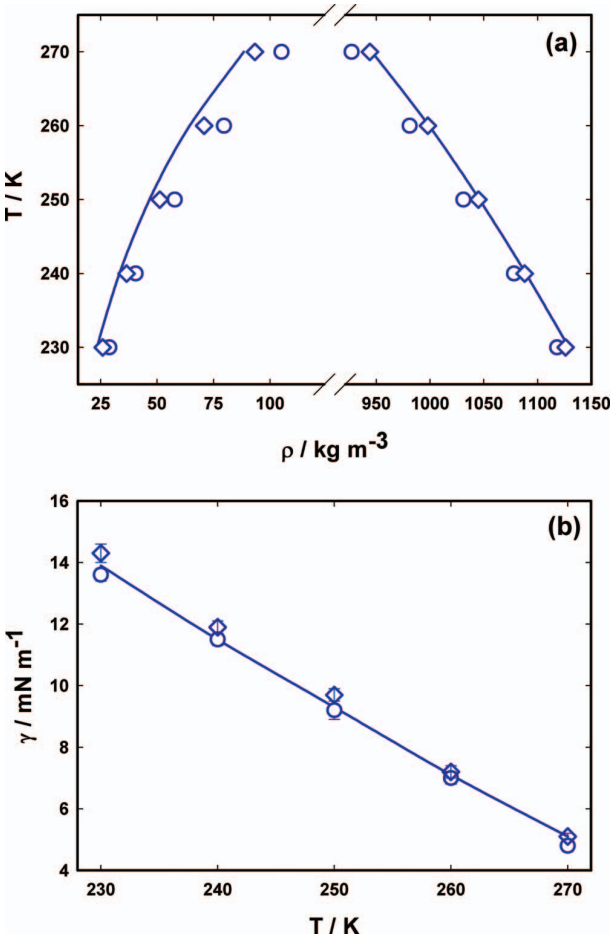

FIG. 3. (a) Coexistence densities for CO_2. Solid line: NIST experimental correlation, symbols: results obtained with the ZD molecular model (circles: calculation without LRCs and $r_c = 5\sigma$, diamonds: calculation with Janeček's LRCs). (b) same caption for interfacial tension, calculated in every case using the TA method.

charges that mimic the existence of a strong quadrupole moment value. Table VII presents the results obtained for the vapour-liquid coexisting densities, and Table VIII those corresponding to the surface tension. In both cases, the range of temperatures studied goes from 230 up to 270 K. The effect of the LRCs, due to the dispersive interactions, accounted for using the Janeček's methodology is clearly noticeable for the case of vapour-liquid coexisting densities. This can be clearly seen in Fig. 3(a) for the case of the ZD model, a fact that is not surprising if we take into account that each molecule contains now three LJ sites. Agreement between predictions from the model and experimental data taken from the literature is better when using the Janeček's inhomogeneous LRCs than with the use of a constant cutoff for the LJ potential and no further corrections. Notice that the last choice produces considerable deviations between simulation and experiment, especially as the temperature is raised. The effect of LRCs, due to the dispersive interactions, on the interfacial tension data is similar to that exhibited in the case of methane, as can be seen in Fig. 3(b). The interfacial tension values obtained from simulation when using the inhomogeneous LRCs are 5% higher than those corresponding to the case in which a constant value of the cutoff distance is used. As a result, the simulations that use a constant cutoff distance for the intermolecular potential overestimates the experimental data in the whole range of temperatures considered.

TABLE VIII. Simulation data of surface tension (γ/ mJ m^{-2}), for the different CO_2 molecular models tested.

T/K	$\gamma_{ta}^{\text{NO-LRC}}$	γ_{ta}^{LRC}	$\gamma_{ta}^{\text{NO-LRC}}$	γ_{ta}^{LRC}	γ^{NIST}[50]
	MSM		EPM2		
230	14.0(3)	14.6(2)	13.9(3)	14.2(3)	13.9
240	11.7(2)	12.1(3)	11.7(2)	12.0(2)	11.5
250	9.0(2)	9.9(2)	9.2(2)	9.6(3)	9.3
260	7.1(2)	7.4(3)	6.9(1)	7.4(2)	7.1
270	5.0(1)	5.3(2)	4.8(2)	5.1(2)	5.1
	TraPPE		ZD		
230	15.0(3)	15.9(2)	13.6(2)	14.3(3)	13.9
240	12.9(3)	12.4(2)	11.5(2)	11.9(2)	11.5
250	10.7(2)	11.1(2)	9.2(3)	9.7(2)	9.3
260	8.1(2)	8.4(2)	7.0(2)	7.2(2)	7.1
270	5.7(2)	6.1(1)	4.8(2)	5.1(1)	5.1

V. CONCLUSIONS

We have studied the effect of LRCs, due to the dispersive interactions, on the surface tension of several molecular models of real substances. The results shown in this work lead to the following conclusions. First, the pure truncation of the dispersive (LJ) term of the intermolecular potential produces an undesirable underestimation of the computed interfacial tension along biphasic inhomogeneous Monte Carlo simulations. This effect has been checked for models where the LJ term represents the complete intermolecular potential contribution, as it is the case for the typical united-atom methane forcefield, but also for models including point electric charges in their molecular structures, as it is the case of TIP4P-type models for water or MSM-type models for carbon dioxide. In every case, the complete account of LRCs using the Janeček's methodology, with the improved formulation of MacDowell and Blas, leads to an augmentation around 5%-7% on the values of the interfacial tension for the pure fluids investigated. Additionally, this methodology allows a faster convergence on the determined interfacial tension and coexistence densities from cutoff distance values as short as 3σ. Moreover, this method is superior to post processing methods as the determination of the integrated contribution to the interfacial properties due to potential truncation. The variation on the properties produced by dispersive LRCs treatment must be taken into account for quantitative purposes when comparing the respective performances of different models parametrizations. In addition, the use of this methodology circumvents the otherwise necessary heuristic and non rigorous choice of the cutoff distance, which plays an important role also beyond the pure numerical results, because it also imposes the use of large simulation boxes. This latter condition, added to the inherent slowness of this type of biphasic simulations and combined with the fact that simulation times increase very fast with the cutoff distance, allows to conclude that the use of the dispersive potential tail correction as proposed in this work optimizes the formal reliability, numerical performance, and CPU time requirement of the calculation of interfacial properties.

ACKNOWLEDGMENTS

The authors acknowledge CESGA (www.cesga.es), for providing access to computing facilities, and Consellería de Educación e Ordenación Universitaria (Xunta de Galicia) and Ministerio de Ciencia e Innovación (Grant Nos. FIS2009-07923, FIS2010-14866, and FIS2012-33621, and FPU Grant No. AP2007-02172 for J.M.M.), in Spain, for financial support. Further financial support from Proyecto de Excelencia de la Junta de Andalucía (Grant No. P07-FQM02884) and Universidad de Huelva are also acknowledged.

[1] J. M. Míguez, M. C. dos Ramos, M. M. Piñeiro, and F. J. Blas, J. Phys. Chem. B **115**, 9604 (2011).
[2] T. Lafitte, B. Mendiboure, M. M. Piñeiro, D. Bessières, and C. Miqueu, J. Phys. Chem. B **114**, 11110 (2010).
[3] C. Miqueu, J. M. Míguez, M. M. Piñeiro, T. Lafitte, and B. Mendiboure, J. Phys. Chem. B **115**, 9618 (2011).
[4] G. A. Chapela, G. Saville, S. M. Thompson, and J. S. Rowlinson, J. Chem. Soc., Faraday Trans. **73**, 1133–1144 (1977).
[5] E. M. Blokhuis, D. Bedeaux, C. D. Holcomb, and J. A. Zollweg, Mol. Phys. **85**, 665–669 (1995).
[6] M. Guo and B. C.-Y. Lu, J. Chem. Phys. **106**, 3688–3695 (1997).
[7] C. Ibergay, A. Ghoufi, F. Goujon, P. Ungerer, A. Boutin, B. Rousseau, and P. Malfreyt, Phys. Rev. E **75**, 051602 (2007).
[8] A. Ghoufi, F. Goujon, V. Lachet, and P. Malfreyt, J. Chem. Phys. **128**, 154716 (2008).
[9] A. Ghoufi, F. Goujon, V. Lachet, and P. Malfreyt, Phys. Rev. E **77**, 031601 (2008).
[10] F. Biscay, A. Ghoufi, F. Goujon, and P. Malfreyt, J. Phys. Chem. B **112**, 13885–13897 (2008).
[11] F. Biscay, A. Ghoufi, F. Goujon, V. Lachet, and P. Malfreyt, J. Chem. Phys. **130**, 184710 (2009).
[12] F. Biscay, A. Ghoufi, and P. Malfreyt, J. Chem. Phys. **134**, 044709 (2011).
[13] J. Janeček, J. Phys. Chem. B **110**, 6264–6269 (2006).
[14] L. G. MacDowell and F. J. Blas, J. Chem. Phys. **131**, 074705 (2009).
[15] M. Mecke, J. Winkelmann, and J. Fischer, J. Chem. Phys. **107**, 9264–9270 (1997).
[16] M. Mecke, J. Winkelmann, and J. Fischer, J. Chem. Phys. **110**, 1188–1194 (1999).
[17] K. C. Daoulas, V. A. Harmandaris, and V. G. Mavrantzas, Macromol. **38**, 5780 (2005).
[18] J. Janeček, H. Krienke, and G. Schmeer, J. Phys. Chem. B **110**, 6916–6923 (2006).
[19] V. K. Shen, R. D. Mountain, and J. R. Errington, J. Phys. Chem. B **111**, 6198–6207 (2007).
[20] J. Janeček, J. Chem. Phys. **131**, 124513 (2009).
[21] J. Benet, L. G. MacDowell, and C. Menduiña, J. Chem. Eng. Data **55**, 5465 (2010).
[22] P. J. in 't Veld, A. E. Ismail, and G. S. Grest, J. Chem. Phys. **127**, 144711 (2007).
[23] J. Alejandre and G. A. Chapela, J. Chem. Phys. **132**, 014701 (2010).
[24] J. M. Míguez, D. G. Salgado, J. L. Legido, and M. M. Piñeiro, J. Chem. Phys. **132**, 184102 (2010).
[25] D. Moller, J. Oprzinsky, and J. Fischer, Mol. Phys. **75**, 1455 (1992).
[26] M. G. Martin and J. I. Siepmann, J. Phys. Chem. B **102**, 2569 (1998).
[27] C. S. Murthy, K. Singer, and I. R. McDonald, Mol. Phys. **44**, 13 (1981).
[28] D. Moller and J. Fischer, Fluid Phase Equilib. **100**, 35 (1994).
[29] C. S. Murthy, S. F. Oshea, and I. R. M. Donald, Mol. Phys. **50**, 531 (1983).
[30] J. G. Harris and K. H. Yung, J. Phys. Chem. **99**, 12021 (1995).
[31] J. J. Potoff and J. I. Siepmann, AIChE J. **47**, 1676 (2001).
[32] Z. Zhang and Z. Duan, J. Chem. Phys. **122**, 214507 (2005).
[33] W. L. Jorgensen, J. Chandrasekhar, J. Madura, R. W. Impey, and M. Klein, J. Chem. Phys. **79**, 926 (1983).
[34] H. W. Horn, W. C. Swope, J. W. Pitera, J. D. Madura, T. J. Dick, G. L. Hura, and T. Head-Gordon, J. Chem. Phys. **120**, 9665 (2004).
[35] J. L. F. Abascal and C. Vega, J. Chem. Phys. **123**, 234505 (2005).
[36] D. Frenkel and B. Smit, *Understanding Molecular Simulation* (Academic, 2002).
[37] E. de Miguel and G. Jackson, J. Chem. Phys. **125**, 164109 (2006).
[38] G. J. Gloor, G. Jackson, F. J. Blas, and E. de Miguel, J. Chem. Phys. **123**, 134703 (2005).
[39] F. J. Blas, L. G. MacDowell, E. de Miguel, and G. Jackson, J. Chem. Phys. **129**, 144703 (2008).
[40] C. Vega and E. de Miguel, J. Chem. Phys. **126**, 154707 (2007).
[41] G. Galliero, M. M. Piñeiro, B. Mendiboure, C. Miqueu, T. Lafitte, and D. Bessières, J. Chem. Phys. **130**, 104704 (2009). P. Orea, Y. Reyes-Mercado, and Y. Duda, Phys. Lett. A **372**, 7024 (2008).
[42] J. M. Míguez, M. M. Piñeiro, A. I. M.-V. Bravo, and F. J. Blas, J. Chem. Phys. **136**, 114707 (2012).
[43] J. Alejandre, D. Tildesley, and G. A. Chapela, J. Chem. Phys. **102**, 4574 (1995).
[44] A. Trokhymchuck and J. Alejandre, J. Chem. Phys. **111**, 8510 (1999).
[45] U. Setzmann and W. Wagner, J. Phys. Chem. Ref. Data **20**, 1061 (1991).
[46] G. R. Somayajulu, Int. J. Thermophys. **9**, 559 (1988).
[47] W. Wagner and A. Pruss, J. Phys. Chem. Ref. Data **31**, 387 (2002).
[48] H. J. White, Jr. *Physical Chemistry of Aqueous Systems: Proceedings of the 12th International Conference on the Properties of Water and Steam* (Orlando, Fl, 1994), Vol. **a107-a138**.
[49] R. Span and W. Wagner, J. Phys. Chem. Ref. Data **25**, 1509 (1996).
[50] W. Rathjen and J. Straub, *Heat Transfer in Boiling* (Academic, New York, 1977).
[51] R. de Gregorio, J. Benet, N. A. Katcho, F. J. Blas, and L. G. MacDowell, J. Chem. Phys. **136**, 104703 (2012).